24th Mediterranean Conference on Control and Automation (MED)
June 21-24, 2016, Athens, Greece

Design, Modelling and Control of a Single Rotor UAV

O. C. Carholt, E. Fresk, G.Andrikopoulos and G. Nikolakopoulos

Abstract— **In this article, a novel Vertical Take-Off and Landing (VTOL) Single Rotor Unmanned Aerial Vehicle (SR-UAV) will be presented. The SRUAV's design properties will be analysed in detail, with respect to technical novelties outlining the merits of such a conceptual approach. The system's model will be mathematically formulated, while a cascaded P-PI and PID-based control structure will be utilized in extensive simulation trials for the preliminary evaluation of the SR-UAV's attitude and translational performance.**

I. INTRODUCTION

The area of Unmanned Aerial Vehicles (UAVs) equipped with a Vertical Take-Off and Landing (VTOL) capabilities has received a constant increase of research interest during the last decade [1][2], mainly due to the important advantages of excluding the need for take-off runways, as well as their low cost design approach. Furthermore, in the general field of VTOLs, there have been multiple designs with the most dominant ones to be those of a) multirotors [3] and b) tilt rotors/wings [4], each providing different mechanical merits in their translational and hovering capabilities. A different approach of a single rotor VTOL design has been researched in the past decades, which bases its operation on the operational principle of thrust vectoring via the utilization of a single propeller and control fins [5][6]. This specific type of UAV has the merit of simplifying the design process, while keeping the development cost to a minimum, thus increasing their applicability in real life applications, while rendering them as a promising alternative aircraft solution to existing VTOL micro-UAV designs.

From a design point of view, the main functional characteristic, of a Single Rotor UAV (SR-UAV), is the utilization of four rectangular airfoils, usually called control fins, which are placed symmetrically at the bottom of the aircraft and directly beneath the propeller. The fins are attached to servo actuators that are used to adjust the angle of attack and produce torque around all the principal axes, thus enabling for a controllable attitude. A three-dimensional visualization of the proposed design is presented in Fig. 1.

In general, the design approaches for SR-UAVs have a long history as a concept. Specifically, in the 1950s and 1960s experimental VTOL aircraft's, such as the Convair XFY Pogo [7] and the Lockheed XFV [8] have been developed that possessed the ability of taking off and landing on their tail, then tilt horizontally for forward flight, commonly known as a tail-sitter [9]. However, their utilization have been proven impractical because of several issues, such as their difficulty in landing due to the pilots' visual restriction, even if in the proposed tail-sitting SR-UAV designs this limitation is not encountered as the vehicle will be operated autonomously.

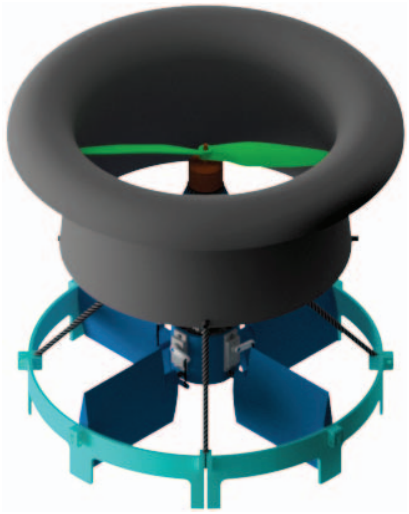

Fig. 1. Conceptual design of the SR-UAV, equipped with a ducted propeller, four actuated fins, as well as structural and landing support.

Tail-sitter UAVs, similar to the presented SR-UAV, have been also utilized in the cases of military surveillance missions and inspection of disaster sites, such as the damaged Fukushima Dai-Ichi nuclear power station, where the Honeywell RQ-16A T-Hawk was utilized [10]. An advantage of the SR-UAVs, when compared to counter rotating propeller and multi-rotor based designs, is a reduction in complexity, i.e. no gearbox, less motors/propellers that in turn lead to less points of failure and a more economical solution [11]. In addition, a ducted propeller leads to a higher efficiency [12], while it is safer to operate and has a lower chance of human injuries during the operation. On the contrary, an inherent issue that describes the SR-UAVs, is the fact that in such designs the propellers create a torque on angular acceleration of the vehicle, which leads to a rotation that needs to be counteracted to achieve a stable yaw [13].

The main novelty of this article is triple. Firstly, a novel design of a single rotor UAV will be presented and analysed. Secondly, a theoretical model that describes the attitude and translation problem of the UAV will be formulated, and finally a novel control structure that is utilizing four control fins to counter the angular momentum and to control the

The authors are with the Control Engineering Group, Department of Computer Science, Electrical and Space Engineering, Luleå University of Technology, SE–97187, Luleå, Sweden

This work has partially received funding from the European Unions Horizon 2020 Research and Innovation Programme under the Grant Agreement No.644128, AEROWORKS.

Corresponding Author's email: geonik@ltu.se

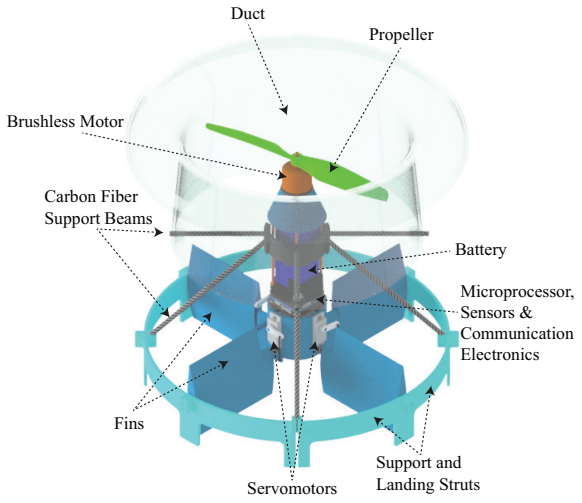

Fig. 2. Main components of the SR-UAV.

attitude of the vehicle will be established.

The rest of the article is structured as follows. In Section II, the proposed single rotor design is presented, while in Section III a system model around hovering is derived. Section IV presents the control scheme development, while Section V presents multiple simulations that prove the efficiency of the proposed scheme, Finally, in Section VI the conclusions are drawn.

II. Design of the Single Rotor UAV

In Fig. 2 a graphical representation of the proposed SR-UAV is presented with the main components of the SR-UAV highlighted. The airframe consists of an inner core, which holds the avionics and the carbon fiber support struts, which in turn connect the core with a fan duct and the four control fins. A structural support for the suspension rod, on which the control fins are rigidly fitted, was designed to act as landing struts. The SR-UAV design properties can be divided into three sub-systems: a) the avionics, b) the propulsion, and c) the flight control, which will be analysed in the sequel.

A. Avionics

From a conceptual point of view, an on-board flight computer system can be utilized to output the five control signals: a) one to control the thrust of the motor, and b) four for torque control via regulating the motion of the control fins. The microprocessor is used to run the angular rate control loop, while incorporating an Inertial Measurement Unit (IMU) as feedback. The flight computer is also communicating with a ground-station that is executing the translational/position control loop, with position data fed back by a motion capture system, without the need of additional on-board sensors at this phase of design. The Li-Po battery pack is properly placed on the centre-axis so as to not contribute any imbalance.

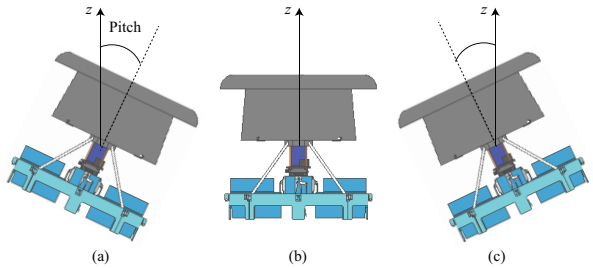

Fig. 3. SR-UAV operation states: (a) Acceleration, (b) Hovering, and (c) Deceleration.

B. Propulsion

The SR-UAV is designed to be actuated by an outrunner brushless DC motor that drives the propeller in a pulling configuration. A duct is proposed in this design for increasing the thrust, while lowering noise when operating at hover or near hover states, as well as to increase the overall safety of operating the SR-UAV in populated areas. However, the proper placement of the duct is a mechanical detail of high importance in order to contribute in performance over the resulting increase in weight [12]. The design parameters, regarding the duct design, have been inspired from [12].

C. Flight Control

The required torque is generated via the use of four control fins, which are located symmetrically around the center-axis of the main body. The reason behind the incorporation of a symmetrical airfoil is to get same behaviour at both positive and negative Angle of Attack (AoA). The fins are designed to be replaceable and therefore different profiles will be utilized in future experimental tests. Other possible conceptual considerations would include the use of a cambered airfoil, since the fins will be tilted to counteract the induced torque from the propeller, which will be addressed in future work.

Similarly to multirotors, forward flight is achieved by pitching in order to direct the acceleration vector as presented in Fig. 3. The same principle is utilized to move sideways by the rolling action. In this article and for the preliminary evaluation of this novel concept, the flight envelope is constrained to small angles in roll and pitch, so as to limit the translational speed and keep the SR-UAV structurally bounded and closer to the hover state.

III. System Modelling

In this Section, the modelling analysis of the proposed SR-UAV is mathematically formulated. Given the geometrical representation of the exerted forces and the respective torques on the design presented in Fig. 4, the model of the system is derived by studying the Newton-Euler equations of a rigid body[14] as:

$$\begin{pmatrix} \boldsymbol{F} \\ \boldsymbol{\tau} \end{pmatrix} = \begin{pmatrix} m\boldsymbol{I}_{3x3} & 0 \\ 0 & \boldsymbol{I}_{cm} \end{pmatrix} \begin{pmatrix} \boldsymbol{a}_{cm} \\ \dot{\boldsymbol{\omega}} \end{pmatrix} + \begin{pmatrix} 0 \\ \boldsymbol{\omega} \times (\boldsymbol{I}_{cm}\boldsymbol{\omega}) \end{pmatrix}, \quad (1)$$

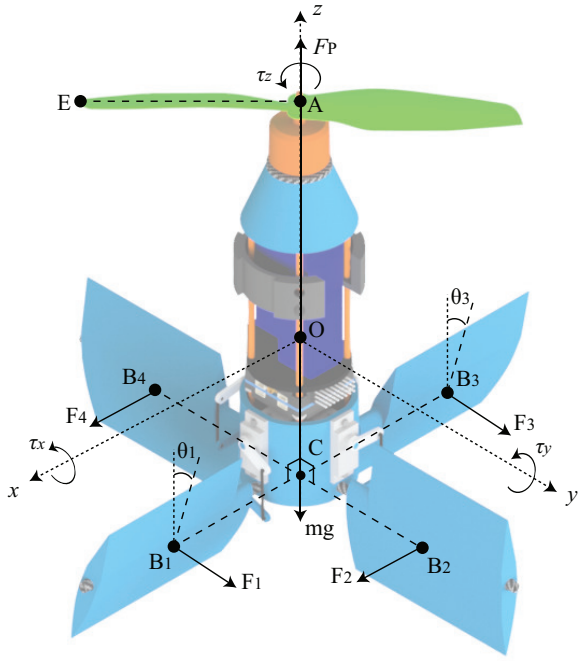

Fig. 4. Acting force diagram of the SRUAV's body frame. Where the distances $(OC) \coloneqq L$,$(CB) \coloneqq r$, and $(AE) \coloneqq R$.

where $\boldsymbol{F} = \begin{bmatrix} F_x & F_y & F_z \end{bmatrix}^T \in \mathbb{R}^3$ is the force acting on the centre of mass, $\boldsymbol{\tau} = \begin{bmatrix} \tau_x & \tau_y & \tau_z \end{bmatrix}^T \in \mathbb{R}^3$ is the torque around the cetre of mass, $\boldsymbol{\omega} = \begin{bmatrix} \omega_x & \omega_y & \omega_z \end{bmatrix}^T \in \mathbb{R}^3$ is the angular velocity, $\boldsymbol{a}_{cm} = \begin{bmatrix} a_x & a_y & a_z \end{bmatrix}^T \in \mathbb{R}^3$ is the acceleration of the centre of mass, $\boldsymbol{I}_{3x3}$ is the 3x3 identity matrix and $\boldsymbol{I}_{cm} = \begin{bmatrix} I_{xx} & I_{xy} & I_{xz} \\ I_{yx} & I_{yy} & I_{yz} \\ I_{zx} & I_{zy} & I_{zz} \end{bmatrix} \in \mathbb{R}^{3x3}$ the inertia matrix. The left hand side of equation 1 can be expanded as:

$$\begin{pmatrix} F_x \\ F_y \\ F_z \\ \tau_x \\ \tau_y \\ \tau_z \end{pmatrix} = \begin{pmatrix} F_2 + F_4 \\ F_1 + F_3 \\ F_P \\ \tau_1 + \tau_3 \\ -\tau_2 - \tau_4 \\ -\tau_P + \tau_1 - \tau_2 - \tau_3 + \tau_4 \end{pmatrix} + m\boldsymbol{R}_g, \tag{2}$$

in relation to the acting force diagram in Fig. 4 where $\boldsymbol{R}_g = \begin{bmatrix} g_x & g_y & g_z & 0 & 0 & 0 \end{bmatrix}^T \in \mathbb{R}^6$ is the gravitational acceleration exerted on the body frame and m the is the mass. Additionally, the effect of aerodynamic forces on the UAV's body is considered negligible when operating in hover or near hover states.

The Propeller force F_P is modelled as follows:

$$F_P = K_{force} u^2. \tag{3}$$

were K_{force} is the maximum force generated by the propeller and u the motor's input.

By assuming that the SR-UAV operates at small angles, the Angle of Attack (AoA) for each fin is equal to its corresponding fin angle (θ_i) and the force generated by the fins can be described in terms of the lift equation as presented below:

$$L = \frac{1}{2} C_l \rho V^2 A, \tag{4}$$

where C_l is the coefficient of lift, $\rho [kg/m^3]$ is the air density, $V [m/s]$ is the true airspeed and $A [m^2]$ is the surface area of the wing. All terms except V are assumed to be constant and can be approximated to the term K_{force}. The airspeed can in turn be expressed as proportional to the propeller force F_P and the component of the fin angle (θ) that lies in the X-Y-plane $(sin(\theta))$. The force generated by each fin thus becomes:

$$F_i = sin(\theta_i) K_{force} u^2. \tag{5}$$

The fin torque (τ_i) may now be described as the appropriate lever times the fin force (F_i) and the motor torque as a torque constant (K_{torque}) times the motor force. In this way, the kinematics of the system in the body frame is formulated:

$$\begin{pmatrix} F_x \\ F_y \\ F_z \\ \tau_x \\ \tau_y \\ \tau_z \end{pmatrix} = \begin{pmatrix} 0 & 0 & 1 & 0 & 1 \\ 0 & 1 & 0 & 1 & 0 \\ 1 & 0 & 0 & 0 & 0 \\ 0 & L & 0 & L & 0 \\ 0 & 0 & -L & 0 & -L \\ -K_{torque} & r & -r & -r & r \end{pmatrix} \begin{pmatrix} 1 \\ s\theta_1 \\ s\theta_2 \\ s\theta_3 \\ s\theta_4 \end{pmatrix} K_{force} u^2 + m\boldsymbol{R}_g. \tag{6}$$

where $s\theta_i = sin(\theta_i)$. Finally, the solution of the Newton-Euler equations in (1) with respect to the translational and angular accelerations yields the equations of motion:

$$\begin{pmatrix} a_x \\ a_y \\ a_z \\ \dot{\omega}_x \\ \dot{\omega}_y \\ \dot{\omega}_z \end{pmatrix} = \begin{pmatrix} (s\theta_2 + s\theta_4) K_{force} \frac{u^2}{m} \\ (s\theta_1 + s\theta_3) K_{force} \frac{u^2}{m} \\ K_{force} \frac{u^2}{m} \\ (s\theta_2 + s\theta_4) L \cdot K_{force} \frac{u^2}{I_{xx}} - \omega_x^2 \\ (s\theta_1 + s\theta_3) L \cdot K_{force} \frac{u^2}{I_{yy}} - \omega_y^2 \\ (-K_{torque} + s\theta_1 - s\theta_2 - s\theta_3 + s\theta_4) r \cdot K_{force} \frac{u^2}{I_{zz}} - \omega_z^2 \end{pmatrix} + \boldsymbol{R}_g, \tag{7}$$

which will be utilized in section V as the body frame model of the SR-UAV.

IV. CONTROL

In this Section, the control problem involving all the Degrees of Freedom (DOFs) for the SR-UAV, namely the translational $[x, y, z]^T$ and the attitude $[\phi_x, \phi_y, \phi_z]^T$, will be addressed.

For controlling the translational DOFs, the conventional ProportionalIntegralDerivative (PID) controller [15] was utilized (Fig. 5). The PID controller is one of the most utilized model-free control algorithms, featuring a feedback control action $u(t)$, which utilizes the weighted sum of three control parameters, namely, a proportional term, an integral term, and a derivative term, and for the translational controllers can be mathematically formulated as in:

$$u_i(t) = K_{P,i} e_i(t) + K_{I,i} \sum_{a=1}^{b} e_i(t_a) \Delta t + K_{D,i} \frac{e_i(t_b) - e_i(t_{b-1})}{\Delta t}, \tag{8}$$

where K_p, i is the proportional gain, $K_{I,i}$ is the integral gain and $K_{D,i}$ is the derivative gain, with $i = 1, 2, 3$ the index for the corresponding translational controllers.

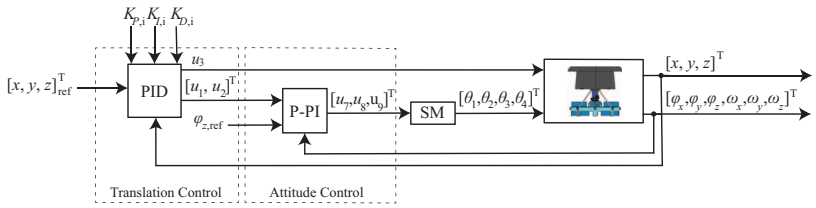

Fig. 5. PID and cascaded P-PI structure for the respective control of the translation and attitude performance of the SR-UAV.

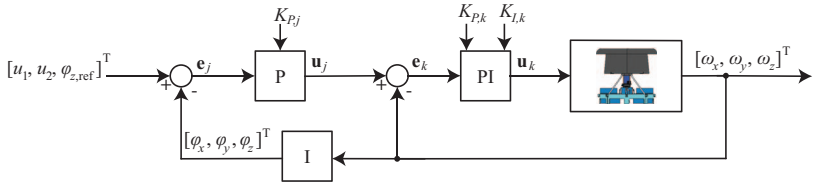

Fig. 6. Cascaded P-PI structure for attitude control.

By an appropriate selection of the aforementioned control parameters, the controllers goal is to adjust the manipulated variable $u_i(t)$ and achieve minimization of the respective error signal $e_i(t) = (w_{i,ref} - w_i)$, where $(w_1, w_2, w_3) = (x, y, z)$, i.e. equivalence between the set-point value $x_{ref}, y_{ref}, z_{ref}$ and the process value x, y, z. The manipulated variables u_i define the control efforts of the PIDs, where $u_1 = \phi_{x,ref}$ and $u_2 = \phi_{y,ref}$ are the reference inputs for the attitude P-PI controllers, while $u_3 = \phi_{z,ref}$ is the motor control signal for the SR-UAV.

Furthermore, a set of cascaded proportional-proportional-integral (P-PI) controllers (Fig. 6) is utilized to control the SR-UAV's attitude. Similar to the PID, every cascaded P-PI features an inner loop containing the proportional and integral terms, and an outer loop featuring a proportional controller, which is placed in an outer loop. As it has been presented in[3], in which the use of a P^2-controller was addressed, with such a cascade control formulation, the attitude on quadrotors can be successfully controlled. In the case of the SR-UAV, the integral was added to accommodate the induced torque from the propeller. The PI and P controllers can be mathematically formulated as in:

$$u_j(t) = K_{P,j} e_j(t), \tag{9}$$

$$u_k(t) = K_{P,k} e_k(t) + K_{I,k} \sum_{a=1}^{b} e_j(t_a) \Delta t, \tag{10}$$

where in (9), $K_{p,j}$ is the proportional gain of the outer loop, $e_j(t)$ is the reference defined as $e_j(t) = ((u_2 - \phi_x), (u_3 - \phi_y), (\phi_{z,ref} - \phi_z))$, where $\phi_{z,ref}$ is the reference yaw angle, which is independent of the translational controllers, and $j = 4,5,6$ is the index range used for identifying the outer loop controllers. The manipulated variable $u_j(t)$ serves as the input for the inner loop (10), where $K_{p,k}$ is the proportional gain of the inner loop, $K_{I,k}$ is the integral gain, and $k = 7,8,9$ is the index used for identifying the inner loop controllers. The reference $e_k(t)$ is defined as $e_k(t) = ((u_4 - \omega_x), (u_5 - \omega_y), (u_6 - \omega_z))$, where the manipulated variable $u_k(t)$ involves the control signals used for the control fins of the SR-UAV which are given by:

$$\begin{aligned} \theta_1 &= u_7 + u_9 \\ \theta_2 &= -u_8 - u_9 \\ \theta_3 &= u_7 - u_9 \\ \theta_4 &= -u_8 + u_9. \end{aligned} \tag{11}$$

Equation (11) is executed by the signal mixer block (SM) in Fig. 5.

V. Preliminary Evaluation

The overall closed-loop system described in section IV was simulated in order to provide a preliminary evaluation of the behaviour of the proposed design as well as the efficiency of the utilized control structure. The simulations were executed with a sample-rate of 50Hz. White-noise was added to the outputs of the simulations in order to simulate the resolution of the proposed sensors. Noise was also added in the form of a white-noise sequence $N(\mu, \sigma^2)$ where μ is the mean and σ^2 is the variance, in the position data $n_1 \in N(0,1)mm$, in angle $n_2 \in N(0, 0.0087^2)rad$ and in angular rate $n_3 \in N(0, 0.17^2)rad/s$.

A. Design Parameters

For the simulation of the proposed SR-UAV and in order to extract the parameters needed for it's preliminary evaluation, through the utilization of the aforementioned control scheme, the materials of all parts were properly selected. Specifically, all structural and support parts, i.e. the duct, the inner core of the body frame, the control fins, as well as the landing struts, have been properly designed to be 3D printed via polyactide (PLA) plastic for decreased weight and high endurance. A suitable choice for constructing the profile of the fins would be the airfoil type NACA0020. The last two digits in the NACA profile was chosen to get a relative thin profile but at the same time accommodate the radius of the suspension rod.

The parameters utilized in the simulated system of the SR-UAV, most of which were extracted through the corresponding Computer Aided Design (CAD), are presented

in Table I. Of these parameters: a) the lengths L and r, as well as the propeller radius R were user defined in the CAD design, b) the mass m and inertia parameters were extracted from the CAD design, and c) the maximum force K_{force} and torque K_{torque} constants were chosen for the purpose of the evaluation that will be presented in the next Section.

TABLE I

DESIGN PARAMETERS OF THE SR-UAV.

Parameter	Value	Units
L	0.106	m
r	0.084	m
R	$0.203 \cdot 10^{-3}$	m
m	0.393	Kg
I_{xx}	$3.7 \cdot 10^{-3}$	$Kg \cdot m^2$
I_{yy}	$3.7 \cdot 10^{-3}$	$Kg \cdot m^2$
I_{zz}	$2.1 \cdot 10^{-3}$	$Kg \cdot m^2$
I_{xy},I_{xz},I_{yz}	~ 0	$Kg \cdot m^2$
K_{force}	15	N
K_{torque}	0.5	Nm

At this point, it has to be noted that the user-defined parameters L and r were properly defined for the purposes of this preliminary evaluation, while R was selected via commercially available propeller dimensions. Further analysis on the effect of alternating the aforementioned parameters is considered as future work and will not be investigated further.

B. Control Parameters

The controller gains where tuned via trial-and-error sequences so as to minimise the settling time and the corresponding oscillations of the closed-loop system. The gains utilized for the simulation results, are listed in Table II.

C. Simulation Results

A simulated response of the system via set-point reference signals for the closed-loop translational movement of the SR-UAV is presented in Fig. 7. Furthermore, in Fig. 8 the resulting attitude responses for the roll, pitch and yaw DOFs are being presented. In this case, the control goal is for the angle responses to track the reference signals (tracking problem). From the obtained results, it is obvious that the responses in all the axes of motion, reveal successful set-point tracking, with small rising times for the set-point references and absence of intense transient phenomena for all the cases despite the effect of the added noise signals into the system, which has a larger impact on the angle reference signals $\phi_{x,ref}$ and $\phi_{y,ref}$.

TABLE II

CONTROL PARAMETERS FOR EACH DOF OF THE SR-UAV.

Gain	Values		
$K_{P,i}$	0.04	0.04	1
$K_{I,i}$	0.001	0.001	1
$K_{D,i}$	0.1	0.1	0.5
$K_{P,j}$	1.3	1.3	2.5
$K_{P,k}$	0.02	0.02	0.02
$K_{I,k}$	0.02	0.02	0.02

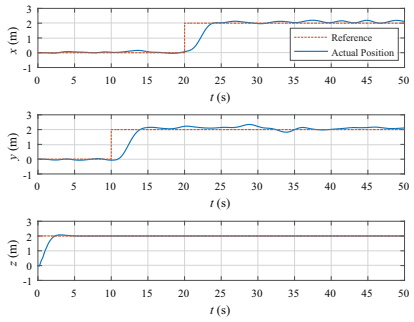

Fig. 7. Translational step-response of the SR-UAV.

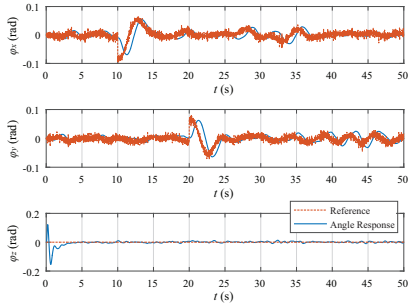

Fig. 8. Attitude response induced by a translational step of the SR-UAV.

TABLE III

THE ROOT MEAN SQUARE ERROR (RMSE) OF THE STEADY STATE ERROR IN THE STEP-RESPONSE SIMULATION

D.O.F	RMSE
x	0.1065 m
y	0.1417 m
z	0.0013 m
ϕ_x	0.0114 rad
ϕ_y	0.0130 rad
ϕ_z	0.0042 rad

Furthermore, these responses reveal that the SR-UAV possesses the design characteristics for achieving successful translational and attitude performance, combined with the utilization of the proposed P-PI and PID control scheme, which is proved to be a suitable choice for this system.

This can be further supported from the extracted root mean square errors (RMSE) of the aforementioned responses, presented in Table III. This criterion reveals that low RMSE values of the closed-loop system remain in generally small values, especially for the cases of the z axis, where the error is kept in the order of 0.001 m, and the ϕ_i signals that remain to the order of 0.001 rad. The oscillations in x and y, as well as the larger RMSE value, reveal the limitations of the control structure into counteracting the effect induced by the noise.

In Fig. 9 a graph showing the tracking performance of the suggested modeling and control scheme for a helix path following simulation is depicted for a simulation time of 150s. From the obtained results it is obvious that the system is capable of following a path with similar oscillations, as in the case of step responses, while the control scheme can

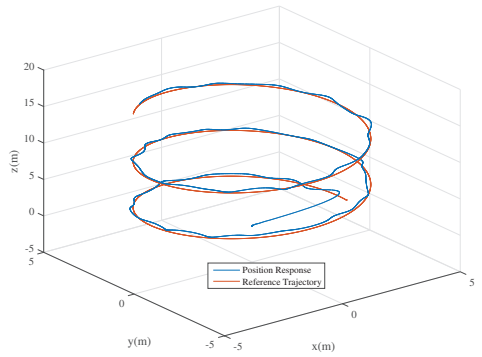

Fig. 9. The SR-UAV system's response, while tracking a helix-shaped trajectory.

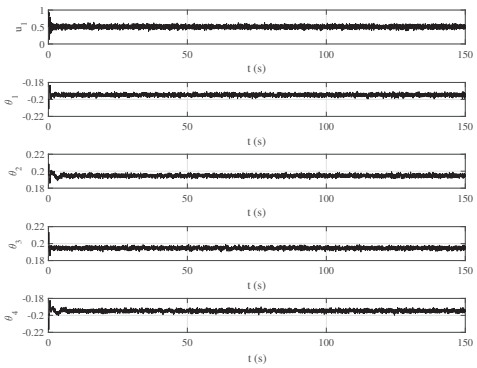

Fig. 10. The SR-UAV control signals, while tracking a helix-shaped trajectory.

track a rather fast 3-dimensional varied set-point. In this type of simulations, it has been also noted that the slower this variation is (bigger the helix is) the better the achievable tracking can be. It has been indicated in Table IV, the RMSE of the presented tracking response reveals no significant change in the ϕ_x,ϕ_y,ϕ_z and z over the steady state of the step response. Finally, in Fig. 10 the simulated motor and servomotor signals are presented as the helix trajectory is followed.

TABLE IV

THE ROOT MEAN SQUARE ERROR (RMSE) OF THE HELIX SIMULATION

D.O.F	RMSE
x	0.7326 m
y	0.6777 m
z	0.0013 m
ϕ_x	0.0125 rad
ϕ_y	0.0125 rad
ϕ_z	0.0039 rad

VI. CONCLUSIONS

In this article, the design, modeling and control of a Single-Rotor UAV (SR-UAV) was presented. The conceptual design stages of the SR-UAV were analyzed in detail, with respect to the advantages of utilizing a single rotor-based structure for the future development of a low-cost and safe UAV with VTOL capabilities. The model was mathematically formulated for the hovering case, which was utilized in the simulation of the closed-loop system, with a control system based in cascaded P-PI and PID controllers to undertake the problem of tranlational and attitude control. The simulated responses revealed that the SR-UAV possessed the design characteristics for achieving successful translational and attitude tracking, combined with the utilization of the proposed P-PI and PID control scheme, which was proved to be a choice that can lead such a system to smooth and accurate tracking performances.

Future work includes the utilization of alternative tuning techniques to further improve the control behaviour of the proposed design, as well as the implementation and testing of more sophisticated controllers, e.g. optimal control algorithms, so as to achieve higher accuracy in more demanding tracking scenarios. The final ultimate goal of the presented research is to develop the SR-UAV prototype and test it extensively in various experimental conditions.

REFERENCES

[1] K. Alexis, G. Nikolakopoulos, A. Tzes, and L. Dritsas, "Coordination of helicopter uavs for aerial forest-fire surveillance," in *Applications of intelligent control to engineering systems*, pp. 169–193, Springer, 2009.

[2] K. Alexis, G. Nikolakopoulos, and A. Tzes, "On trajectory tracking model predictive control of an unmanned quadrotor helicopter subject to aerodynamic disturbances," *Asian Journal of Control*, vol. 16, no. 1, pp. 209–224, 2014.

[3] E. Fresk and G. Nikolakopoulos, "Full quaternion based attitude control for a quadrotor," in *European Control Conference (ECC), July 17-19, 2013, Zurich, Switzerland*, 2013.

[4] A. Lindqvist, E. Fresk, and G. Nikolakopoulos, *Optimal Design and Modeling of a Tilt Wing Aircraft*, pp. 701 – 708. IEEE, 2015.

[5] S. Bose, R. Verma, K. Garuda, A. Tripathi, and S. Clement, "Modeling, analysis and fabrication of a thrust vectoring spherical vtol aerial vehicle," in *Aerospace Conference, 2014 IEEE*, pp. 1–6, March 2014.

[6] S. Avinash, V. Aravind, J. Ananthapadmanabhan, P. Dinesh, K. Aditya, B. Shankar, N. Sheryas, and J. Freeman, "Innovative dynamic stability control for vtols using thrust vectoring," in *Information and Automation for Sustainability (ICIAFs), 2010 5th International Conference on*, pp. 317–322, Dec 2010.

[7] B. Yenne, *Convair Deltas from SeaDart to Hustlerl.* Specialty Press: North Branch, 2009.

[8] J. Winchester, *Lockheed XFV-1 Salmon. Concept Aircraft: Prototypes, X-Planes and Experimental Aircraft.* Kent, UK: Grange Books plc, 2005.

[9] F. J. Allen, "Bolt upright: Convair's and lockheed's vtol fighters," *Air Enthusiast (Key Publishing)*, vol. 127, p. 1320, 2007.

[10] E. Guizzo, "Robotic aerial vehicle captures dramatic footage of fukushima reactors."

[11] K. G. Wernicke, "The single-propeller driven tailsitter is the simplest and most efficient configuration for vtol uavs,"

[12] J. L. Pereira, *Hover and wind-tunnel testing of shrouded rotors for improved micro air vehicle design.* ProQuest, 2008.

[13] Z. C. D. Zhang and J. Lv, "Lift system design of tail-sitter unmanned aerial vehicle," *Intelligent Control and Automation*, vol. 3, no. 4, pp. 285–290, 2012.

[14] H. Hahn, *Rigid Body Dynamics of Mechanisms.* Springer., 2002.

[15] Bennett, *A History of Control Engineering, 18001930.* Stevenage, U.K.: IET: IEE Control Engineering, 1986.